Biophysical Chemistry 7 (1977) 299–309

EQUILIBRIUM GEL PERMEATION: MEASUREMENT OF SOLUTE PARTITIONING BY DIRECT FLUORESCENCE SCANNING‡

Leland P. VICKERS and Gary K. ACKERS*
Department of Biochemistry, University of Virginia, Charlottesville, Virginia 22901, USA

Received 23 December 1976

The feasibility of using fluorescence detection in quantitative gel permeation measurements has been explored. It is shown that the effect of scattering by the gel matrix can be evaluated in terms of pathlength-dependent turbidity functions for excitation and emission wavelengths. Experimental studies were carried out to evaluate these functions in cross-linked dextran gels (Sephadexes) and in agarose gels (Sepharoses). Empirical turbidity functions derived for these gels have a simple form, leading to accurate simplifying approximations for the scattering correction required in a fluorescence gel permeation measurement. Using this approach, partition cross-sections were estimated for dansyl-conjugated β-gamma globuline and for dansyl-conjugated bovine serum albumin. The results establish feasibility of the method and clearly indicate the instrumentation requirements for its accurate implementation.

1. Introduction

The technique of direct optical scanning of gel chromatography columns, originally introduced by Brumbaugh and Ackers [1], has been usefully applied in the study of interacting protein systems [2–6] and offers considerable potential for further development. An equilibrium method based upon this approach [7, 8] requires that the column be completely saturated with a solution containing the molecular species of interest. The column is then scanned by being driven through a horizontally collimated beam of light and absorbance values are determined as a function of distance. The molecular size-dependent partitioning properties of the solute are thus determined at ~400 points along the column axis. Even with the small columns employed (10 ml bed volume) the procedure requires relatively large volumes of sample, especially if a series of concentrations is to be investigated. An alternative approach consists of saturating a very small flow cell packed with gel beads (bed volume less than one ml) with the solution of interest and monitoring the absorbance of this cell and a corresponding reference cell containing the same solution but no gel. A single-photon counting instrument was built for this purpbse and has been described in a previous publication from this laboratory [9]. The sample carriage in this instrument has four positions: The first one (a) is an air reference; (b) and (c) are two gel-packed flow cells, and (d) is a reference flow cell. The three cells are connected in series so that buffer or a sample solution can be pumped through them. Measurement of absorbances in these cells provides a determination of the partition cross section, ξ. This fundamental parameter is the fraction of cross-sectional area occupied within the gel bed, and is a measure of solute molecular size [1,10]. The partition cross-section for a given solute is obtained simply as the quotient of the solution absorbance measured above the gel background and the absorbance of the same solution in the gel-packed flow cell [9].

An alternative to absorbance measurements for the detection and quantitation of solutes in such experiments is fluorescence. Proteins may be detected by the intrinsic fluorescence of their aromatic groups [11,12] or by the emission of a fluorescent molecule which has become attached to the protein. These may

‡ Supported by USPHS grant GM 14493. This work constitutes part of the Ph.D. dissertation presented by Leland P. Vickers in May 1976.
* To whom correspondence should be addressed.

be covalently or non-covalently bound "reporter groups" of fluorescent ligands involved in functional properties of the protein. A fluorescent label has been used to monitor the elution of proteins from a 4% agarose column in the presence of sodium dodecylsulfate for molecular weight determinations [13].

The purpose of this investigation was to explore the feasibility of using fluorescence detection to measure partitioning of solutes within porous gel networks. Because of the high sensitivity of fluorescence detection, the technique should permit studies to be carried out below the concentration range presently accessible through absorbance measurements. Additionally the errors in a fluorescence measurement will be less than that of a corresponding absorbance measurement, at a given sensitivity of radiant intensity measurement. This results from the fact that in absorbance measurements concentration is proportional to the logarithm of the intensity, whereas in fluorescence measurements it is linearly proportional (at low concentrations) to intensity.

First we will present the mathematical relationships necessary in the determination of partition cross-sections from fluorescence intensity measurements. A major point of concern is to evaluate the effects of scattering by the gel network on the measurements. Hence, we will present results of a study of this scattering by several commonly-employed chromatographic gels. Next, the application of fluorescence detection to the determination of partition cross-sections for two fluorescently-labeled proteins will be given. Finally, some possibilities for future developments and applications will be discussed.

2. Background and quantitative relationships

2.1. Fluorescence instrumentation

The three basic geometries commonly used for fluorescence measurements include the right-angle, frontal, and in-line configurations [cf. 14]. The most widely applicable is the right-angle geometry, whereas solutions of high optical density (whether because of absorption of scattering) are usually measured by the frontal method. The in-line method requires a means of discriminating between excitation light and emission light since unlike the other two methods a large component of the measured intensity may consist of the unabsorbed portion of the excitation light. The in-line method has been explored in greatest detail in these studies since the photon counting instrument used was built for absorbance measurements and therefore has this geometry [9].

Although the in-line method is the least desirable for fluorescence measurements, it is the most desirable for the studies of pathlength-dependent turbidity in gel beds, which are a necessary prerequisite to the interpretation of all measurements of fluorescence within such systems.

In a fluorescence measurement the excitation light is unidirectional, whereas the fluorescence is emitted in all directions. Therefore, the measured intensity represents some solid angle of the entire sphere of radiation. This gives rise to a geometrical efficiency term which varies from zero to unity, but could only approach unity with an integrating sphere detector. The development of lasers and stable xenon arc lamps of high intensity has made possible the measurement of weakly fluorescing solutions, even with low geometrical efficiencies.

For the absorbance measurements made with the photon-counting spectrophotometer [9] an interference filter is placed between the sample and the photomultiplier tube to reduce stray light. In order to use the instrument for fluorescence measurements this filter is replaced by another interference filter which discriminates between the excitation and emission wavelengths. With the monochromator set at the excitation wavelength an ideal filter would block out all light of this wavelength not absorbed by the sample, but would have good transmission characteristics at the emission wavelength.

However, the observed intensity is the sum of the fluorescence intensity and any intensity at the excitation wavelength which has "leaked" through the filter:

$$I_{obs}^{sample} = F + I_{leak}. \quad (1)$$

The second term on the right side of eq. (1) is

$$I_{leak} = I_0 (T_{total}) T_x, \quad (2)$$

where T_{total} is the product of the transmittance of the sample, T_{sam}, and of the baseline, T_{base}, and T_x is the transmittance of the filter at the excitation wavelength.

For a cuvet containing buffer solution only, the measured intensity will be

$$I_{obs}^{buf} = I_0 (T_{base})\, T_x, \tag{3}$$

assuming the buffer is not fluorescent. The first term on the right side of eq. (1) is

$$F = \phi' (I_{abs})\, T_m, \tag{4}$$

where I_{abs} is the absorbed intensity, T_m is the transmittance of the filter at the emission wavelength, and ϕ' is the product of the quantum efficiency and geometrical efficiency terms. The absorbed intensity is

$$I_{abs} = (1 - T_{sam})\, I_0. \tag{5}$$

Combining eqs. (1) and (2) gives

$$I_{obs}^{sample} = F + I_0 (T_{total})\, T_x. \tag{6}$$

Substituting eq. (3) into (6) and rearranging gives

$$F = I_{obs}^{sample} - I_{obs}^{buf} (T_{sam}). \tag{7}$$

Alternatively, eq. (6) can be normalized with respect to I_0,

$$I_{obs}^{sample}/I_0 = F/I_0 - (T_{total})\, (T_x).$$

Rearrangement gives

$$F/I_0 = T_{obs} - (T_{total})\, (T_x), \tag{8}$$

where $T_{obs} = I_{obs}^{sample}/I_0$, is the apparent transmittance of the sample.

Fluorescence intensity can therefore be expressed either as in eqs. (7) or (8). If I_0 changes with time then eq. (8) is clearly preferred.

At low concentrations, where T_{sam} approaches unity, eq. (7) can be approximated as

$$F = I_{obs}^{sample} - I_{obs}^{buf}.$$

This approximation can be similarly made in eq. (8).

2.2. *Correction factors for fluorescent measurement in a scattering medium*

The fluorescence of a sample is proportional to the intensity of light absorbed. For the sample of fig. 1:

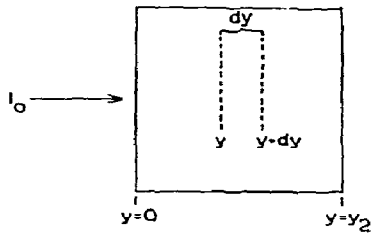

Fig. 1. The sample cell. I_0 is the incident intensity at $y = 0$; y_2 is the cell pathlength; y is any particular distance from the cell's inner face, $y = 0$.

$$F = \phi [I_0 (1 - e^{-\epsilon c y_2})], \tag{9}$$

where I_0 is the excitation intensity at $y = 0$, ϵ is the absorptivity of the solution, C is the concentration, and ϕ is the quantum efficiency (with a value between zero and unity). A derivation of this relationship is presented in the appendix. If the quantity $\epsilon c y_2$ is small the following approximation can be made,

$$F \approx \phi I_0 \epsilon c y_2; \tag{10}$$

therefore, the fluorescence intensity is linearly proportional to concentration. This is seen to be the case for dilute solutions [15].

For concentrations which exceed the linear fluorescence range it is common practice to correct the measured fluorescence, F, to the expected linear fluorescence F_0 by the following formula,

$$F_0 = F \left(\frac{\epsilon c y_2}{1 - e^{-\epsilon c y_2}} \right). \tag{11}$$

These corrections are usually termed "inner-filter corrections". An equation similar in form can be found in most references on fluorescence measurement and is usually given as:

$$F_0 = F \left(\frac{2.3\ (\text{O.D.})\, y_2}{1 - T^{y_2}} \right),$$

where T and O.D. are the transmittance and optical density of the sample at 1 cm pathlength.

A second complication, and one which is of great significance in measurements carried out in the presence

of gel beads, is the effect of scattering. The optical density of a scattering medium may be expressed as a function of pathlength by a "turbidity function", $\tau(y)$. This function may be different for the excitation and emission wavelengths, represented as $\tau_x(y)$ and $\tau_m(y)$, respectively.

A total concentration of solute, c', will be used when referring to measurements in the presence of gels. This is distinguished from the bulk concentration, c. The relationship between them is: $c' = \xi c$ [cf. ref. 10].

All the derivations presented here are based upon the assumption that scattering effects are completely uncoupled from absorption (inner-filter) effects. This has been found to be the case with Sephadex gels (cross-linked dextran beads) within the limits of experimental measurement [1].

The expression for the amount of light absorbed within an increment dy is (see appendix):

$$I_y - I_{y+dy} = I_y(1 - \bar{e}^{\epsilon c' dy}),$$

where

$$I_y = I_0\, \bar{e}^{\epsilon c' y}\, e^{-\tau_x(y)}.$$

(the term $e^{-\tau_x(dy)}$ does not appear in this expression because it represents the scattering within the increment dy not absorption, and therefore does not contribute to the fluorescence.)

For integration $dy \to 0$, and the resulting expression is

$$I_y - I_{y+dy} = I_0\, e^{-[\epsilon c' y + \tau_x(y)]}\, \epsilon c' dy.$$

The fluorescence intensity is also attenuated by scattering of the gel matrix. Another term must therefore be included in the integral to account for this effect. The fluorescent intensity becomes:

$$F = \phi \int_0^{y_2} I_0\, e^{-[\epsilon c' y + \tau_x(y)]}\, \epsilon c' dy\, e^{-\tau_m(y_2 - y)}, \quad (12)$$

where $(y_2 - y)$ is the pathlength of emission from the increment dy at a distance y.

A correction for combined inner-filter and inner-scattering effects would be:

$$F_0 = F\left(\frac{\epsilon c' y_2}{\int_0^{y_2} e^{-[\epsilon c' y + \tau_x(y) + \tau_m(y_2 - y)]}\, \epsilon c' dy}\right). \quad (13)$$

In general the functions $\tau_x(y)$ and $\tau_m(y)$ must be found experimentally and eq. (12) is then integrated numerically. A simpler procedure based upon the experimental results of this study will be described.

3. Experimental methods

3.1. Optical characterization of the gels

The scattering characteristics of a number of gels were studied as a function of pathlength and wavelength in the ultraviolet and visible regions. Effects of variation in bead size and porosity were also explored. For all except the pathlength studies, a quartz cuvet of 5 mm pathlength was used. The gels used were Sephadexes G-25 Fine (70 μM dia), G-25 Medium (130 μM dia), G-25 Coarse (270 μM dia), G-25 Superfine (20 μM), G-100 Medium and G-200 Medium, and Sepharoses 4B and 6B (Pharmacia Fine Chemicals). A more complete description of these gels can be found in ref. [10]. The Sephadex gels were swollen in deionized water and were rinsed and decanted a number of times. The Sepharose gels were similarly rinsed.

Cuvets of gel were allowed to gravity pack overnight before optical density measurements were made. Insignificant changes were observed in the optical density in the period between 3 hours after packing and 2 days. The gel beds were found to pack reproducibly as evidenced by the optical density. The cuvets were masked on the detector side with standard flow cell masks, each having an opening of 1.5 × 6 mm. Some experiments were done with the cuvet fronts also masked but no differences were observed in the results between these experiments and those without masks on the front.

Experiments were carried out between wavelengths of 220 nm and 600 nm. The slit width varied between 0.001 mm in the visible region and 0.03 mm in the low ultraviolet region. No effect of varying slit width in this range was observed on the optical densities. The slit height of the monochromator (Zeiss MQ4III) is slightly less than 1 cm. A deuterium lamp was used as the source. Counting rates were always less than 10^6 s^{-1}.

A water baseline was taken in each case in the cell

with the same masking as used for the corresponding gel measurement. These baselines were subtracted from the optical densities measured with the gels present.

For the pathlength studies a set of plexiglass cuvets were constructed with pathlengths between 0.16 and 1.27 cm. They were painted black except for a window on each side, 1.5 × 6 mm. The absorption characteristics of plexiglass limited their use to wavelengths greater than 350 nm. Also used were quartz cuvets of pathlength 0.1, 0.2, 0.5, and 1.0 cm, masked in the same way as mentioned above.

3.2. Filter selection

Preliminary experiments were carried out using proteins conjugated with dansyl chloride (1-dimethylaminonaphthalene-5-sulfonyl chloride) so a filter was used which would allow light to pass in the 500 nm region but would block out light in the 350 nm region. Representative emission and excitation spectra can be found in ref. [16]. Such a filter would also be suitable for proteins conjugated with N-dansylaziridine [17].

An interference filter specially made for these studies (Infrared Industries, Waltham, Massachusetts) had a half-peak bandwidth of 10 nm, centered at 500 nm. The transmittance at 500 nm was 0.505 (50.5%) and at 350 nm was 3.4×10^{-6}, making the discrimination between the two wavelengths greater than 10^5.

3.3. Fluorescence measurements

Three fluorescent proteins were used for the studies: fluorescamine-conjugated bovine serum albumin, dansyl-conjugated bovine serum albumin, and dansyl-conjugated bovine gamma-globin. The fluorescamine-BSA was prepared with Fluram (Roche Diagnostics) and the dansyl-conjugated proteins were prepared by a method of Weber [10]. Approximately 4 dansyl/groups were conjugated to each protein in these preparations.

All measurements were obtained using a 0.5 cm pathlength. The solution measurements were made in quartz cells and the flow system measurements were made in a set of flow cells described in a publication from this laboratory [9]. The 500 nm interference filter was used for both fluorophores. The fluorescamine-BSA was excited at 400 nm and the dansyl-conjugated proteins at 350 nm. Fluorescamine-BSA has an emission peak at about 475 nm which is sufficiently broad to have considerable intensity in the 500 nm region. Counting times were usually 1000 s, since the intensity was very low. The dark count normally was $5\ s^{-1}$ with a standard error of 0.1 and was subtracted from measured intensities.

The partitioning experiments were carried out using Sephadex G-200 (lot 8063) and 0.1 M potassium phosphate, pH 7.3, plus 0.15 M NaCl as the buffer.

4. Results

4.1. Optical characterization of the gels

Fig. 2A shows the effect of varying porosity (degree of crosslinking) on beds of Sephadex gel at a number of wavelengths. Three gels are shown, all with approximately the same bead size. The one with the largest pore size (i.e., lowest volume fraction of cross-linked dextran), G-200, was found to scatter light the least. The curve shapes are characteristic of all Sephadex gels studied. The optical density was found to change slowly in the visible region and to increase in the ultraviolet region. Fig. 2B shows the same effects for Sephrose gels. Again, the gel with the larger pore size, 4B, scattered light the least. The most noticeable difference was the pronounced slope in the visible region.

The effect of varying bead size is seen in fig. 3. The gels used were G-25 coarse, medium, and fine. The optical density of G-25 superfine was higher than G-25 fine, but was measured with such a large uncertainty that it is not shown. The gel with the largest bead size scattered light the least.

Fig. 4A is a plot of optical density versus pathlength, l, at two wavelengths in the visible: 400 nm and 500 nm. The equation represented by the solid line will be discussed below. Data points from both the quartz and plexiglass cuvets are shown. Fig. 4B is a similar plot for three wavelengths in the ultraviolet: 200 nm, 300 nm, 350 nm.

Attempts were made to fit the data to a second order polynomial constrained to go through the origin:

$$a(\text{O.D.})^2 + b(\text{O.D.}) = l.$$

The coefficient of the linear term was usually very small in comparison to the quadratic term. In a fluorescence experiment the optical density of the gel will be known only for the pathlength of the gel flow cell. For

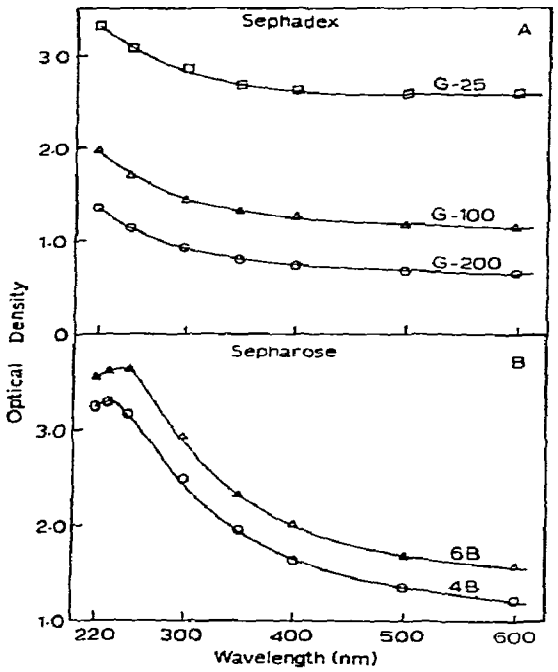

Fig. 2. Effect of porosity on the optical density of gel beds. Pathlength is 5 mm. A. Sephadex gels: ○, G-200 Medium; △, G-100 Medium; □, G-25 Medium. B. Sepharose gels: ○, 4B; △, 6B.

this reason, and because the linear term was very small in the fit mentioned above, the data was fitted to only one parameter:

$$\text{O.D.} = p(l)^{1/2}. \tag{14}$$

The coefficient, p, was determined by the method of linear least squares:

$$p = \sum(l)^{1/2}\,(\text{O.D.}) \sum[(l)^{1/2}]^2. \tag{15}$$

The line drawn by this method was found to fit the data well in all cases, except for points at the shortest pathlengths. There is a systematic deviation in this region, but judging by the scatter in the other points it is within experimental error. The estimated values of p are summarized in table 1.

A 0.5 cm flow cell was packed with Sephadex G-100 (Medium) and allowed to flow for 2 days after which optical density measurements were made at a

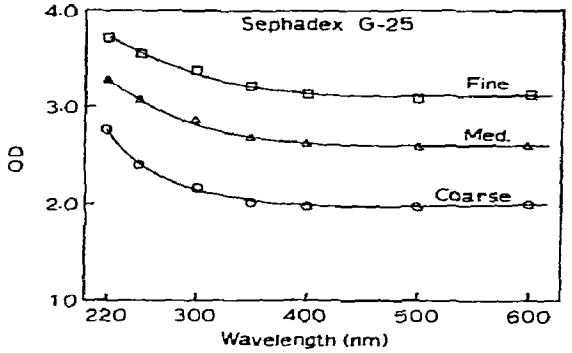

Fig. 3. Effect of bead size on the optical density of Sephadex gels. Pathlength is 5 mm. ○, G-25 Coarse; △, G-25 Medium; □, G-25 Fine.

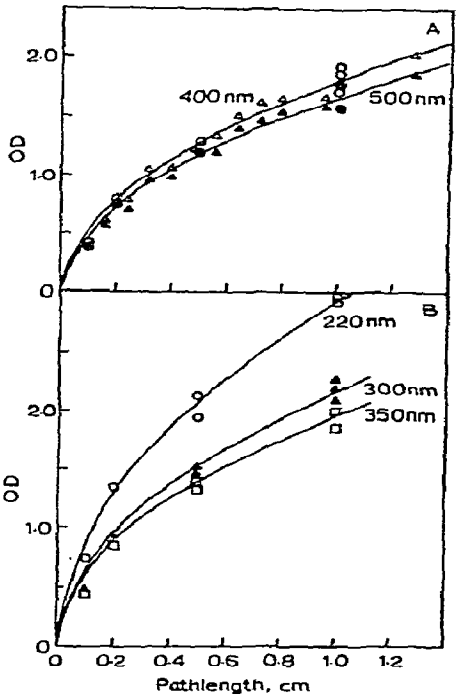

Fig. 4. Optical density of Sephadex G-100 Medium in cells of various pathlength. A. Visible wavelength region: ○, quartz cells at 400 nm; △, plexiglass cells at 400 nm; ●, quartz cells at 500 nm; ▲, plexiglass cells at 500 nm. The solid lines are the best fit to O.D. = $p\sqrt{l}$. p = 1.81 for 400 nm and p = 1.67 for 500 nm. B. Ultraviolet wavelength region: (all cells were quartz) ○, 220 nm; ▲, 300 nm; □, 350 nm. The solid lines are the best fit to O.D. = $p\sqrt{l}$. p = 2.92 for 200 nm, 2.15 for 300 nm, and 1.94 for 350 nm.

Table 1
Values of p in the equation (O.D.) = $p(l)^{1/2}$ for pathlength dependence data for Sephadex G-100

Wavelength (nm)	p a)
220	2.92
300	2.15
350	1.94
400	1.81
500	1.67

a) p was determined by eq. (19).

number of wavelengths. The optical densities were found to be slightly higher than those of the 0.5 cm gravity-packed gel, whereas the wavelength dependence curve had the same qualitative features.

4.2. Simulations

In order to explore the inner filter and gel scattering effects a series of simulations were carried out corresponding to the experimental conditions of this study.

Fluorescent intensities were calculated according to eqs. (9) and (10) for a 0.5 cm pathlength. In these estimates no value of ϕI_0 was assumed, so the values calculated were $F/\phi I_0$. Eq. (9) was found to deviate from the linear approximation eq. (10) as expected [15]. A 1% deviation was found at an absorbance of 0.02.

Based upon the good fit of eq. (14) to the experimental optical densities of gel-packed cells, we may formulate the following turbidity functions.

$$\tau_x(y) = 1.94(y)^{1/2},$$
$$\tau_m(y) = 1.67(y_2 - y)^{1/2}$$

The numerical integration of eq. (12) was explored using these functions. For these integrations the values of p (table 1) have to be adjusted because of the natural logarithm base in eq. (12).

Subsequently it was found that eq. (12) could be closely approximated by the following relationship:

$$\frac{F}{\phi I_0} = \frac{\int_0^{y_2} e^{-[\tau_x(y)+\tau_m(y_2-y)]}\,dy}{y_2} \times \int_0^{y_2} e^{-\epsilon c' y}\,\epsilon c'\,dy. \qquad (16)$$

The first factor is simply the average of the function

$$e^{-\tau_x(y)+\tau_m(y_2-y)} \qquad (17)$$

across the pathlength y_2, and the second factor is identical to eq. (9). The shape of these two functions from zero to y_2 is shown in fig. 5. At concentrations where the second factor deviates 1% from linearly, the entire approximation of eq. (16) deviates less than 0.05% from the true value of eq. (12). Therefore, in the low concentration range a good approximation is

$$F/\phi I_0 = B\,\epsilon c y_2. \qquad (18)$$

where B is the first factor on the right side of eq. (16).

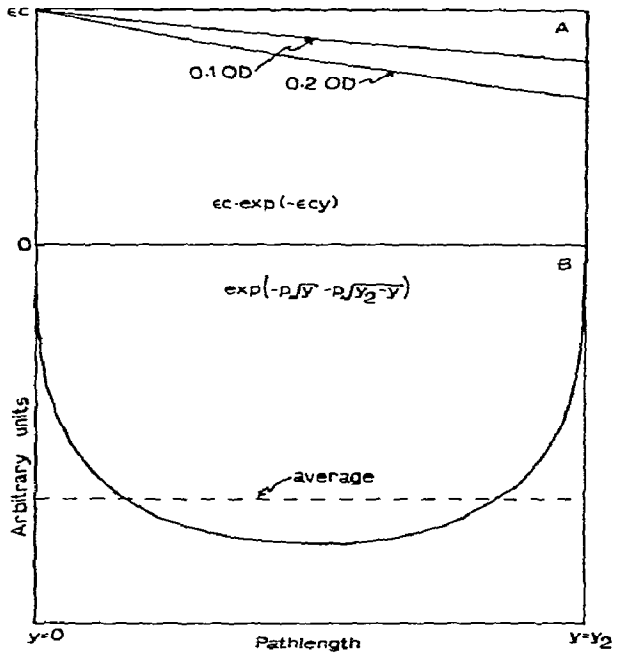

Fig. 5. Graphical representation of the two factors of eq. (16). The abscissa is the pathlength and the ordinates are in arbitrary units. The two curves in A show the deviation from the linear approximation for solutions of optical density 0.1 and 0.2. For dilute solutions the area under the curve is approximated by $\epsilon c y_2$. The curve in B was calculated with equal values of p in τ_x and τ_m. If the values of p were not equal the curve would be slightly skewed. The dashed line is the average value of the function.

For dilute solutions the fluorescence intensity is therefore expected to be linearly proportional to concentration both in the solution flow cell *and in the gel flow cell*:

$$F_a = \phi I_0 \epsilon c y_2, \tag{19}$$

and

$$F_b = \phi I_0 B \epsilon c' y_2 = \phi I_0 B \epsilon \xi c y_2. \tag{20}$$

These two equations can be solved for ξ in terms of the measured fluorescences and B:

$$\xi = F_b / B F_a. \tag{21}$$

The assumption is made that the absorptivity, ϵ, does not change in the gel, a condition verified by the studies of Brumbaugh and Ackers [1].

The standard error in ξ can be calcu..ted from the standard errors in F_b, F_a, and B using the equation for error propagation in a quotient. The error in partition cross-section is

$$\Delta\xi = \xi\left\{\left(\frac{\Delta F_b}{F_b}\right)^2 + \left(\frac{\Delta F_a}{F_a}\right)^2 + \left(\frac{\Delta B}{B}\right)^2\right\}^{1/2} \tag{22}$$

4.3. Fluorescence measurements

The fluorescence intensities of solutions of fluorescamine-BSA were measured with the single-photon spectrophotometer, equipped with the interference filter described in section 3.2. The fluorescence intensity, corrected for inner-filter effects was found to be quite linear despite the fact that the counts were low. A low concentration series was measured with a high incident intensity (1.7×10^9 s^{-1} instead of 9.3×10^5 s^{-1}). These measurements were made on solutions with optical densities down to 0.008. When both sets of data were normalized to the incident intensity, F_0/I_0, the composite plot was linear.

The partitioning of the two dansyl-conjugated proteins into Sephadex G-200 was first measured by the absorbance method [9]. The partition cross section, ξ, for dansyl-BGG was found to be 0.444 ± 0.049 (the solution optical density was 0.0133 for a 0.5 cm pathlength at 350 nm) and for dansyl-BSA it was 0.491 ± 0.020 (optical density 0.102). The partitioning was then measured by fluorescence, and the ξ was determined as discussed in section 4.2. Values of B were estimated independently from the turbidity data and eq. (16). The results are summarized in table 2. The partitioning of the two proteins was done with two different gel-packed flow cells. A small difference in packing accounts for the difference in the values of B.

5. Discussion

The mathematical model used to characterize the scattering of the gels is entirely phenomenological and therefore gives no information as to the structural source of the scattering. However, some generalizations can be made from experiments with the various gel systems. The scattering centers do not appear to be primarily the bead envelope, although there was an effect of bead size. Beuche [19] concluded from light scattering studies of a cylindrical polymeric gel that the scattering was due to the nonuniform swelling of the gel caused by the random character of the crosslink. Both the Sephadex and Sepharose gels exhibited the relationship that the smaller average porosities gave the greater scattering.

The fluorescence was attenuated by the scattering to 20–30% of the value expected in the absence of gel ($B = 0.2$–0.3). This is quite a favorable result compared with the absorption method where the gel baseline is usually greater than 1 O.D. (less than 10% transmittance).

The fluorescence studies we have carried out establish the feasibility of quantitative measurement of partition cross-sections in beds of gel particles and provide the theoretical and experimental background for efficient design of new instrumental systems that will permit studies in the lower concentration ranges. For greater precision, using the present instrument, the absolute number of fluorescence counts would have to be increased. However, this would also increase the number of excitation counts that leak through the filter. Possibly this could be reduced somewhat with a different filter or combination of filters. A discrimination of 10^5 does not appear to be adequate.

The instrument used in these studies was designed for absorbance measurements and is far from ideal for fluorescence applications. The frontal and right-angle methods have been used successfully for measuring fluorescence in other highly scattering media, such as

Table 2
Determination of the partitioning of dansyl-BGG and dansyl-BSA into Sephadex G-200 by fluorescence measurements

	$O.D._{350nm}^{0.5cm}$	I_0 (s^{-1})	F_a (s^{-1})	F_b (s^{-1})	B	ξ [a]
Dansyl-BGG	0.041	5×10^7	35.1 ± 2.8	2.8 ± 0.15	0.207	0.385 ± 0.096
	0.035	2×10^8	119.8 ± 5.5	10.4 ± 0.27	0.206	0.425 ± 0.053
Dansyl-BSA	0.054	2×10^7	16.6 ± 1.7	2.6 ± 0.12	0.291	0.538 ± 0.112
	0.107	2×10^7	44.1 ± 3.2	6.6 ± 0.15	0.287	0.521 ± 0.076

[a] The standard error in ξ was calculated using eq. (22) and assuming the errors in B to be insignificantly small in comparison to those in F_a and F_b.

whole cells or turbid suspensions [12], and would appear to be the methods of choice for gel partitioning experiments. However, the in-line method was necessary for the gel scattering studies.

A method has been reported for monitoring protein bands by fluorescence in acrylamide gels using a right-angle instrument [12]. In that study the intrinsic fluorescence of the protein was used, and a correlation was found between the total amount of protein and the intensity. However, the scattering problems encountered with solid acrylamide gels are not nearly as great as with beaded gels.

For a self-associating protein system, the partition cross section calculated with eq. (21) would be a weight average and therefore would vary with species distribution. Weight-average partition cross sections determined as a function of protein concentration can be analyzed to obtain stoichiometries and association constants. The precise determination of partition cross sections is mandatory for an unequivocal characterization of self-associating systems by gel permeation [7, 8,10].

A combination of the frontal or fight-angle methods and a very stable high intensity source should enable these fluorescence methods to be extended to lower concentrations of fluorophore and to the use of the intrinsic fluorescence of proteins. This would provide the capability of studying protein interactions at concentrations below those now possible with absorption optics using either gel permeation or ultracentrifuge methods. Fluorescence measurement techniques have also been recently applied to analytical ultracentrifugation [20].

The fluorescence of a solute in the presence of a scattering medium would obey the same mathematical form as eq. (12) in either the right-angle or frontal geometries. The parameters of interest are shown in fig. 6. The formula corresponding to eq. (12) for the right-angle geometry is:

$$F = \phi I_0 \int_0^{y_2} e^{-[\epsilon c x_1 + \tau_x(x_1) + \tau_m(y_2 - y)]} \epsilon c dy.$$

For the frontal geometry the relationship is:

$$F = \phi I_0 \int_0^{y_2} e^{-[\epsilon c y + \tau_x(y) + \tau_m(y)]} \epsilon c dy.$$

The methods described here could also be extended to more complex situations, such as when the absorption bands of the fluorophore overlap the emission region.

Determination of partition cross-sections by fluorescence measurement can be used in the study of ligand binding by a simple extension of the method developed by Brumbaugh and Ackers [2,3]. The simple case of the

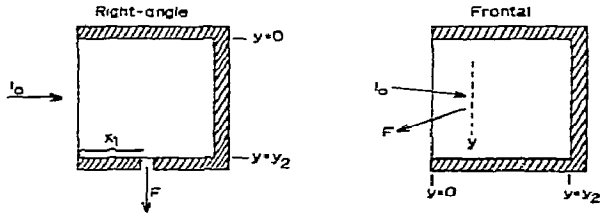

Fig. 6. Configuration of excitation and emission pathways for the right-angle and frontal geometries. In the upper cuvet, x_1 is the distance to a narrow emission slit.

binding of a single fluorescent small ligand, L, to a macromolecule, P, illustrates the method

$$P + L \rightleftharpoons PL.$$

The experimental quantity required for determination of the binding constant is the binding ratio, r, as a function of free ligand concentration [L]:

$$r = ([L_0] - [L])/[P_0],$$

where $[L_0]$ is the total ligand concentration and $[P_0]$ is the total macromolecule concentration. Each mixture can be prepared from stock solutions by weight so that the total concentrations of P and L are accurately known.

A gel is chosen so that the macromolecule and macromolecule–ligand complex are excluded ($\xi_P = \xi_{PL} = \alpha$) and the ligand is completely included ($\xi_L = \alpha + \beta$).

The fluorescence intensity measured from the solution flow cell is

$$F_a = k_P[P] + k_L[L] + k_{PL}[PL],$$

where k_i is the product of a number of constants for species i

$$k_i = \phi_i I_0 \epsilon_i y_2.$$

The fluorescence intensity measured from the gel flow cell is

$$\begin{aligned} F_b &= Bk_P\xi_P[P] + Bk_L\xi_L[L] + Bk_{PL}\xi_{PL}[PL] \\ &= B(k_P\alpha[P] + k_L\alpha[L] + k_L\beta[L] + k_{PL}\alpha[PL]) \\ &= B\alpha F_a + Bk_L\beta[L]. \end{aligned}$$

Hence the free ligand concentration is

$$[L] = \frac{F_b - B\alpha F_a}{Bk_L\beta} = \frac{F_b/B - \alpha F_a}{K_L\beta}.$$

Since the calibration parameters α, β, and B can be determined independently and k_L can be determined by carrying out a fluorescence measurement in the absence of macromolecule, the determination of F_a and F_b enables one to calculate the free ligand concentration and hence the binding ratio. B can alternatively be determined using a solute of known ξ on the particular gel cell to be used for fluorescence and then solving eq. (21). Ideally an instrument that measures both fluorescence and absorbance on the same samples should be employed.

Acknowledgement

We would like to thank Thomas W. Sturgill for the gift of the dansylated proteins.

Appendix

Fig. 1 provides a close look at the sample cell. At a distance y within the sample the Bougeur–Beer Law is written [11]:

$$I_y = I_0 e^{-\epsilon c y}, \tag{A.1}$$

where I_y is the intensity (flux) at position y in photons/s, I_0 is the intensity at $y = 0$, ϵ is the absorptivity of the solution, and c is the concentration. The amount of light absorbed within a small increment dy is equal to the difference between fluxes into and out of the increment: $I_y - I_{y+dy}$. Applying the Bougeur–Beer law over the increment:

$$I_y - I_{y+dy} = I_y - I_y e^{-\epsilon c dy} = I_y(1 - e^{-\epsilon c dy}).$$

By substituting eq. (A.1) into this expression, we have

$$I_y - I_{y+dy} = I_0 e^{-\epsilon c y}(1 - e^{-\epsilon c dy}), \tag{A.2}$$

and letting $dy \to 0$,

$$I_y - I_{y+dy} = I_0 e^{-\epsilon c y} \epsilon c dy. \tag{A.3}$$

By integrating $I_y - I_{y+dy}$ from $y = 0$ to $y = y_2$ one obtains the total absorbed intensity,

$$\begin{aligned} \int_0^{y_2} (I_y - I_{y+dy})\,dy &= \int_0^{y_2} I_0 e^{-\epsilon c y} \epsilon c dy \\ &= I_0(1 - e^{-\epsilon c y_2}). \end{aligned} \tag{A.4}$$

References

[1] E.E. Brumbaugh and G.K. Ackers, J. Biol. Chem. 243 (1968) 6315.
[2] E.E. Brumbaugh and G.K. Ackers, Anal. Biochem. 41 (1971) 543.
[3] G.K. Ackers, in: Methods in Enzymology, Vol. 27, eds. C.H.W. Hirs and S.N. Timasheff (Academic Press, New York, 1973) p. 441.
[4] M.M. Jones, G.A. Harvey and G.K. Ackers, Biophys. Chem. 5 (1976) 327.
[5] M.M. Jones, J.W. Ogilvie and G.K. Ackers, Biophys. Chem. (1976) 5 (1976) 339.
[6] A. Brown and J.K. Zimmerman, Biophys. Chem. 5 (1976) 351.
[7] H.S. Warshaw, Dissertation, University of Virginia, Charlottesville, Virginia (1973).
[8] H.S. Warshaw and G.K. Ackers, Anal. Biochem. 42 (1971) 405.
[9] G.K. Ackers, E.E. Brumbaugh, S.H.C. Ip and H.R. Halvorson, Biophys. Chem. 4 (1976) 171.
[10] G.K. Ackers, in: The Proteins, Third Ed., Vol. 1, eds. H. Neurath and R.L. Hill (Academic Press, New York, 1971) p. 1.
[11] L. Brand and B. Whitholt, in: Methods in Enzymology, Vol. 11, ed. C.H.W. Hirs (Academic Press, New York, 1967) p. 776.
[12] D.M. Easton, H. Lipner, J. Hines and R.C. Leif, Anal. Biochem. 39 (1971) 478.
[13] M.J. Gleason and A.B. Rawitch, Biochem. Biophys. Res. Commun. 57 (1974) 993.
[14] S. Undenfried, Fluorescence Assay in Biology and Medicine (Academic Press, New York, 1962).
[15] C.A. Parker and W.T. Rees, Analyst 85 (1960) 587.
[16] L.S. Gennis, R.B. Gennis and C.R. Cantor, Biochemistry 11 (1972) 2517.
[17] W.H. Scouten, R. Lubcher and W. Baughman, Biochim. Biophys. Acta 336 (1974) 421.
[18] G. Weber, Biochem. J. 51 (1952) 155.
[19] F. Beuche, J. Coll. Inter. Sci. 33 (1970) 61.
[20] R.H. Crepeau, R.H. Conrad and S.J. Edelstein, Biophys. Chem. 5 (1976) 27.